IC/94/48

INTERNATIONAL CENTRE FOR THEORETICAL PHYSICS

ESTIMATION OF STRONG GROUND MOTION AND MICRO-ZONATION FOR THE CITY OF ROME

D. Fäh

C. Iodice

P. Suhadolc

and

G.F. Panza

INTERNATIONAL ATOMIC ENERGY AGENCY

UNITED NATIONS EDUCATIONAL, SCIENTIFIC AND CULTURAL ORGANIZATION

MIRAMARE-TRIESTE

IC/94/48

International Atomic Energy Agency
and
United Nations Educational Scientific and Cultural Organization
INTERNATIONAL CENTRE FOR THEORETICAL PHYSICS

ESTIMATION OF STRONG GROUND MOTION AND MICRO-ZONATION FOR THE CITY OF ROME

D. Fäh, C. Iodice and P. Suhadolc
Istituto di Geodesia e Geofisica, Università degli Studi di Trieste, Trieste, Italy

and

G.F. Panza
International Centre for Theoretical Physics, Trieste, Italy
and
Istituto di Geodesia e Geofisica, Università degli Studi di Trieste, Trieste, Italy.

MIRAMARE – TRIESTE
March 1994

Abstract

A hybrid technique, based on mode summation and finite differences, is used to simulate the ground motion induced in the city of Rome by possible earthquakes occurring in the main seismogenetic areas surrounding the city: the Central Apennines and the Alban Hills. The results of the numerical simulations are used for a first order seismic micro-zonation in the city of Rome, which can be used for the retrofitting of buildings of special social and cultural value. Rome can be divided into six main zones: (1) the edges and (2) the central part of the alluvial basin of the river Tiber; (3) the edges and (4) the central part of the Paleotiber basin; the areas outside the large basins of the Tiber and Paleotiber, where we distinguish between (5) areas without, and (6) areas with a layer of volcanic rocks close to the surface. The strongest amplification effects have to be expected at the edges of the Tiber basin, with maximum spectral amplification of the order of 5 to 6, and strong amplifications occur inside the entire alluvial basin of the Tiber. The presence of a near-surface layer of rigid material is not sufficient to classify a location as a "hard-rock site", when the rigid material covers a sedimentary complex. The reason is that the underlying sedimentary complex causes amplifications at the surface due to resonance effects. This phenomenon can be observed in the Paleotiber basin, where spectral amplifications in the frequency range 0.3-1.0 Hz reach values of the order of 3 to 4.

Introduction

Numerical simulations play an important role in the estimation of strong ground motion. They can provide synthetic signals for areas where recordings are absent and are therefore very useful for engineering design of earthquake-resistant structures and for retrofitting of particularly important buildings. Lateral heterogeneities and sloping layers, commonly present in nature, can cause effects that dominate the ground motion: the excitation of local surface-waves, focusing and defocusing, and resonance effects. In such circumstances, at least two-dimensional techniques are necessary for a realistic estimate of the ground motion.

To include both a realistic source model and a complex structural model of the site of interest, a hybrid method has been developed that combines modal summation and the finite difference technique (Fäh, 1992; Fäh et al., 1993; Fäh et al., 1994). The propagation of the waves from the source up to the local structure at the site is computed with the mode-summation method for plane layered anelastic structures (Panza, 1985; Florsch et al. 1991). The mode-summation method allows us the simulation of the complete incident wavefield in a given phase-velocity frequency band. Explicit finite-difference schemes (Korn and Stöckl, 1982; Virieux, 1986) are then used to simulate the propagation of seismic waves in a two-dimensional model of the local structure. The hybrid method is particularly suitable to compute the ground motion in two-dimensional models of any complexity, and allows us to take into account the source and propagation effects, including local site conditions.

The area of Rome, considered here, is characterized by several sedimentary basins of considerable thickness, which in some parts are covered by volcanic rocks. The area is very vulnerable to earthquakes, as indicated, for example, by the well-documented damage distribution caused by the M_L=6.8 January 13, 1915, Fucino (Italy) earthquake (Ambrosini et al., 1986). In absence of instrumental data in the city of Rome, a numerical simulation of the ground motion due to the January 13, 1915 Fucino earthquake has been compared with

the observed damage distribution (Fäh et al., 1993). The macro-seismic data in Rome shows essentially that the damage is concentrated at the edges of the alluvial basin of the Tiber river; the heavy and intermediate damage are located in that basin. The same distribution of damage can be expected on the basis of the numerical simulations of this event (Fäh et al., 1993). The highest amplifications are observed at the edges of this alluvial basin, and large amplifications can be observed within the Tiber's river bed. The very good correlation between the damage statistic and the ground motion suggests to use the hybrid technique for a micro-zonation of the entire town, which accounts for events expected in other important seismogenetic areas. For this purpose, a series of different numerical simulations of the ground motion are performed, for different source positions and structural models of the Rome area. The results of such computations are then used for the micro-zonation, based on the spectral amplifications expected in the different zones of the city.

Parametrization of the source and of the propagation path

The most important seismogenetic zones (Figure 1) which can cause structural damage in Rome are the Central Apennines (observed maximum intensity in Rome on the Mercalli-Cancani-Sieberg intensity scale (MCS) VII-VIII) and the Alban Hills (observed maximum MCS in Rome VI-VII) (Molin et al., 1986). The source positions (Figure 1) used in this study include (1) the epicenter of the January 13, 1915 Fucino earthquake, (2) the Carseolani Mountains where, from the study of pattern recognition (Caputo et al., 1980), a strong earthquake is expected to occur, and (3) the Alban Hills. The source mechanisms assigned to these earthquakes are the mechanism of the Fucino earthquake (Gasparini et al., 1985) for event 1 and 2, and the mechanism of a recent earthquake in the Alban Hills (Amato et al., 1984) for event 3. The parameters of the focal mechanism of each event are given in Table 1.

The one-dimensional structural models for the region between the source positions and Rome are given in Table 2. These models are used as reference bedrock structures, and, for each seismic source, the ground motion computed with the hybrid method is always compared with that obtained for the related one-dimensional structure.

The position of the cross sections studied is shown in Figure 2 as dashed lines, and the related two-dimensional structural models are shown in Figure 3. They are based on all the available geological and geotechnical information (Ventriglia, 1971; Serva et al, 1986; Funiciello et al., 1987; Boschi et al., 1989; Feroci et al., 1990). Alluvial sediments can be found in two major areas, the river beds of the Aniene and Tiber. The ancient river bed of the Tiber (referred as Paleotiber) is composed by Sicilian clays, sands and gravel. This sedimentary complex is covered by volcanic rocks which have their origin in the Pleistocene volcanic activity (Ventriglia, 1971). The volcanic rocks have greater wave velocities than the underlying sediments (Sicilian), which therefore define a buried low-velocity zone. The surficial layer, consists of compacted fill, and of the foundations of man-made structures. The transition from the alluvial sediments in the Tiber river bed to the compacted clay is characterized by a very high impedance contrast. In Figure 3, the compacted clay is referred as bedrock.

Since the mechanical properties and thickness of the different soils are not well known, we have used different material properties to enhance the reliability of the micro-zonation. This includes: (1) two different models for which the seismic velocities given in Figure 3 are defined at 1Hz and at 30Hz, respectively, and (2) two different models in which the surficial layer of made ground (fill deposits) has a thickness of 5m and 10m, respectively.

Properties of ground motion for the Fucino event

Several ground motion related quantities can be extracted from the synthetic accelerograms obtained from our numerical modelling. The quantities that we consider here are: (1) the relative peak ground acceleration PGA(2D)/PGA(bedrock), (2) the so-called relative Arias intensity W(2D)/W(bedrock), where W is defined as:

$$W = \frac{\pi}{2g} \lim_{t \to \infty} \int_0^t [\ddot{x}(\tau)]^2 \, d\tau \quad ,$$

where x is the ground displacement, and (3) the relative spectral accelerations or spectral amplification Sa(2D)/Sa(bedrock). PGA(2D), W(2D), Sa(2D) indicate, respectively, PGA, W and Sa computed for the two-dimensional models shown in Figure 3, while PGA(bedrock), W(bedrock), and Sa(bedrock) indicate, respectively, PGA, W and Sa obtained for the one-dimensional reference bedrock models given in Table 2.

For each source, in order to remove the effects of the radiation pattern and of the regional propagation, PGA(2D), W(2D), and Sa(2D) are always normalized with respect to the corresponding quantities, PGA(bedrock), W(bedrock), Sa(bedrock), computed in the reference bedrock model at the given source-receiver distance .

For the Fucino event (Event 1), relative PGA and relative Arias intensity, defined by the ratios (PGA(2D)/PGA(bedrock)) and (W(2D)/W(bedrock)), computed for the transverse component of motion (SH-waves), the radial component of motion, and the total P-SV wavefield, are shown in Figure 4. High relative PGA values are observed for locations sitting on unconsolidated sediments (Figure 4a), while relative PGA values are low where the volcanic layer is thick. Relative peaks can be seen at the beginning of the alluvial valley of the Tiber and within the alluvial valley of the Aniene. The peaks and troughs are more evident in the curve representing the relative W values (Figure 4b). There are five relative peaks: two at the edges of the Tiber basin, one within the alluvial valley of the Aniene, a broad peak where the Sicilian low-velocity zone gets close to the surface, and one at the margin of the Paleotiber basin.

The macro-seismic data show essentially that, in Rome, the damage is concentrated in the basin of the Tiber with clear peaks at the edges of the alluvial basin. To quantify this observation, the damage distribution has been projected on the cross section used in the numerical modelling (Fäh et al., 1993). The resulting histogram is shown in Figure 4, which shows that a similar distribution of damage is predicted by our direct numerical simulation.

First order seismic micro-zonation

All the quantities characterizing some aspect of the strong ground motion, like the maximum amplitude, the duration and the Fourier spectrum, provide only a very limited description of the complete ground motion and certainly do not quantify its damage producing potential. A more adequate quantity, especially from the engineering point of view, is the response spectrum (or the spectral amplification) of the earthquake ground motion. Response spectra (for example Sa) are related to the maximum response of a simple oscillator, whose natural period and damping coefficient are varied, excited by a given ground motion.

The results obtained from the modelling of the Fucino event (Figure 4) can be used directly for general micro-zonation purposes. Using as reference the bedrock models given in Table 2, six zones can be distinguished (see Figures 3 and 4): (1) *zone 1* includes the edges of the Tiber river, (2) *zone 2* extends over the central part of alluvial basin of the Tiber, (3) *zone 3* includes the edges of the Paleotiber basin, and (4) *zone 4* extends over the central part of the Paleotiber basin. The *zones 5* and *6* include areas which are located outside the large basins of the Tiber and Paleotiber where we distinguish between areas (5) without and (6) with a layer of volcanic rocks close to the surface. These zones can be recognized also in the sections considered in relation with the events located in the Carseolani Mountains and the Alban Hills, as is shown in Figure 3.

For all the receivers located in each of the six zones defined above, and for all the two-dimensional models, shown in Figure 3, and the studied events, located in Figure 2, we have computed the spectral amplification Sa(2D)/Sa(bedrock). From these values we have then computed the average and the maximum spectral amplification for each given zone, which are shown in Figure 5, for zero damping and 5% damping of the oscillator.

The greatest spectral amplification is observed at the edges of the sedimentary basin of the Tiber river (zone 1), for frequencies between 2.0 and 2.5 Hz. The maximum spectral amplification with respect to the bedrock model varies between 5 and 6, and it is due to the combination of resonance effects with the excitation of local surface waves. The general shape of the maximum and

average spectral amplifications are similar for zone 1 and 2. In the frequency range from 1.0 Hz to 3.0 Hz, the maximum spectral amplification is of the order of 4 and the average spectral amplification is of the order of 2.

Similar observations can be done for the Paleotiber basin (zones 3 and 4), but in a different frequency band (0.4-1.0 Hz). The buried sedimentary complex (Sicilian) causes maximum spectral amplification between 3 and 4, due to resonance effects. These are most pronounced at frequencies around 0.6 Hz. Therefore, the presence of a near-surface layer of rigid material in the Paleotiber basin is not sufficient to classify that area as a "hard-rock site". A correct zonation requires the knowledge of both the thickness of the surficial layer and of the deeper parts of the structure, down to real bedrock. This is especially important in volcanic areas, where pyroclastic material often covers alluvial basins. The maximum spectral amplification is larger at the edges of the Paleotiber basin (zone 3). For frequencies above 1.0 Hz, in the Paleotiber basin (zone 4), the volcanic layer acts as a shield reflecting part of the incoming energy, and the values of the average spectral amplification are smaller than 1.

For the sites in the zones 5 and 6, the maximum and the average spectral amplifications are small for frequencies below 1 Hz. Since the sedimentary cover in these zones is thin, the amplification takes place at frequencies above 1.5 Hz, and changes rapidly from site to site. This rapid variation leads to average values of the order of 1.0-1.5.

Summary and Conclusions

In absence of instrumental data, a realistic numerical simulation of the ground motion, successfully tested against macro-seismic data, is used for the first order micro-zonation of Rome. The highest values of the spectral amplification are observed at the edges of the sedimentary basin of the Tiber, strong amplification are observed in the Tiber's river bed. This is caused by the large amplitudes and long duration of the ground motion due to (1) the low impedance of the alluvial sediments, (2) resonance effects, and (3) the excitation of local surface waves.

From the computation of the spectral amplification, it has been recognized that the presence of a near-surface volcanic layer of rigid material is not sufficient to classify a location as a "hard-rock site", since the existence of an underlying sedimentary complex can cause amplifications due to resonance effects. A correct zonation requires the knowledge of both the thickness of the surficial layer and of the deeper parts of the structure, down to real bedrock. This is especially important in volcanic areas, where lava flows often cover alluvial basins.

Our technique can be applied routinely in micro-zonation studies, and it provides realistic estimates of the ground motion for two-dimensional, anelastic models. Since the geotechnical data are available for several areas, especially in urban environments, the proposed technique provides a scientifically and economically valid procedure for the immediate (no need to wait for a strong earthquake to occur), first order, seismic micro-zonation of any urban area, and is therefore very useful for engineering design of earthquake-resistant structures and for retrofitting of particularly important buildings.

Acknowledgements

We would like to thank ENEA for allowing us the use of the IBM3090E computer at the ENEA INFO BO Computer Center. D.F. has been supported by the Swiss National Science Foundation under Grant Nr. 8220-037189. This study has been made possible by the contracts CNR 91.02692.CT15, CNR 92.00068.CT12, CNR 92.02422.CT15, CNR 92.02867.PF54, and EEC EPOC-CT91-0042, and by MURST (40% and 60%) funds. This research has been carried out in the framework of the ILP Task Group II.4 contributions to the IDNDR project "Physical Instability of Megacities".

References

AMATO, A., B. DE SIMONI and C. GASPARINI (1984): Considerazioni sulla sismicità dei Colli Albani, *Atti del 3° Convegno del Gruppo Nazionale di Geofisica della Terra Solida*, CNR, Roma, Vol. 2, 965-976.

AMBROSINI, S., S. CASTENETTO, F. CEVOLANI, E. DI LORETO, R. FUNICIELLO, L. LIPERI and D. MOLIN (1986): Risposta sismica dell'area urbana di Roma in occasione del terremoto del Fucino del 13 gennaio 1915, Risultati preliminari, *Mem. Soc. Geol. It.*, **35**, 445-452.

BOSCHI, E., M. FEROCI, R. FUNICIELLO, L. MALAGNINI, A. ROVELLI and S. SALVI (1989): Valutazione della risposta sismica in ambiente urbano: risultati per la città di Roma, *Atti del 8° Convegno Gruppo Nazionale Geofisica della Terra Solida*, CNR, Roma, 317-326.

CAPUTO, M., V. KEILIS-BOROK, E. OFICEROVA, E. RANZMAN, I. ROTWAIN and A. SOLOVJEFF (1980): Pattern recognition of earthquake-prone areas in Italy, *Phys. Earth. Planet. Int.*, **21**, 305-320.

FÄH, D. (1992): A hybrid technique for the estimation of strong ground motion in sedimentary basins, *Ph.D. thesis Nr. 9767, Swiss Federal Institute of Technology, Zurich.*

FÄH, D., C. IODICE, P. SUHADOLC and G.F. PANZA (1993): A new method for the realistic estimation of seismic ground motion in megacities: the case of Rome, *Earthquake Spectra*, **9**, No.4, 643-668.

FÄH, D., P. SUHADOLC, ST. MUELLER and G.F. PANZA (1994): A hybrid method for the estimation of ground motion in sedimentary basins; quantitative modelling for Mexico City, *Bull. Seism. Soc. Am.*, **84**, 000-000.

FEROCI, M., R. FUNICIELLO, F. MARRA and S. SALVI (1990): Evoluzione tettonica e paleogeografica plio-pleistocenica dell'area di Roma, *Il Quaternario*, **3**, 141-158.

FLORSCH, N., D. FÄH, P. SUHADOLC and G.F. PANZA (1991): Complete synthetic seismograms for high-frequency multimode SH-waves, *Pageoph*, **136**, 529-560.

FUNICIELLO, R., G. LORIA and S. SALVI (1987): Ricostruzione delle superfici strutturali del sottosuolo della città di Roma, *Atti del 6° Convegno Gruppo Nazionale Geofisica della Terra Solida, CNR, Roma*, 395-415.

GASPARINI, C., G. IANNACCONE and R. SCARPA (1985): Fault-plane solutions and seismicity of the Italian peninsula, *Tectonophysics*, **117**, 59-78.

KORN, M. and H. STÖCKL (1982): Reflection and transmission of Love channel waves at coal seam discontinuities computed with a finite difference method, *J. Geophys.*, **50**, 171-176.

MOLIN D., S. AMBROSINI, S. CASTENETTO, E. DI LORETO, L. LIPERI and A. PACIELLO (1986): Aspetti della sismicità storica di Roma, *Mem. Soc. Geol. It.*, **35**, 439-444.

PANZA, G.F. (1985): Synthetic seismograms: The Rayleigh waves modal summation, *J. Geophysics*, **58**, 125-145.

SERVA, L., A.M. BLUMETTI and A.M. MICHETTI (1986): Gli effetti sul terreno del terremoto del Fucino (13 gennaio 1915); tentativo di interpretazione della evoluzione tettonica recente di alcune strutture, *Mem. Soc. Geol. It.*, **35**, 893-907.

VENTRIGLIA, U. (1971): La geologia della città di Roma, *Amm. Prov. di Roma, Roma*.

VIRIEUX, J. (1986): P-SV wave propagation in heterogeneous media: Velocity-stress finite-difference method, *Geophysics*, **51**, 889-901.

Event Nr.	Location	Source depth [km]	Dip	Rake	Strike-receiver angle
1	Fucino valley	8.00	39°	172°	38°
2	Carseolani Mountains	8.00	39°	172°	38°
3	Alban Hills	3.06	74°	266°	133°

Table 1. Source mechanisms of the events shown in Figure 1.

Thickness (km)	Density (g/cm^3)	P-wave velocity (km/s)	S-wave velocity (km/s)	Q_β
0.09	2.24 (2.21)	2.40 (1.85)	1.29 (1.00)	30 (20)
0.10	2.25	2.50	1.30	30
0.10	2.25	2.80	1.50	30
0.10	2.30	4.00	2.31	100
0.10	2.40	4.10	2.37	100
0.10	2.40	4.20	2.43	100
0.10	2.50	4.30	2.48	100
0.10	2.50	4.40	2.54	100
0.10	2.50	4.50	2.60	100
0.10	2.50	4.60	2.65	100
0.10	2.60	4.70	2.70	100
0.10	2.60	4.80	2.77	100
0.10	2.60	4.90	2.83	100
0.10	2.60	5.00	2.88	100
0.10	2.60	5.20	3.00	100
0.10	2.60	5.40	3.10	100
0.10	2.60	5.60	3.20	100
1.70	2.80	5.70	3.30	100
6.10	2.85	6.00	3.46	100
0.10	2.85	5.89	3.40	100
0.10	2.85	5.80	3.35	100
0.10	2.85	5.71	3.30	100
0.10	2.85	5.54	3.20	100
8.60	2.85	5.40	3.12	100
0.10	2.85	5.49	3.17	100
0.10	2.85	5.63	3.25	100
0.10	2.85	5.71	3.30	100
0.10	2.85	5.89	3.40	100
0.10	2.85	6.06	3.50	100
2.70	2.85	6.20	3.58	300
1.70	2.88	6.50	3.75	300
1.70	2.90	6.70	3.87	300
2.40	2.95	7.00	4.04	300
4.75	3.35	7.90	4.56	300
4.75	3.35	7.92	4.57	300
4.75	3.35	7.94	4.58	300
4.75	3.35	7.96	4.59	300
4.75	3.35	7.98	4.60	300
4.75	3.35	8.00	4.62	300
4.75	3.36	8.02	4.63	300
4.75	3.37	8.04	4.64	300
4.75	3.38	8.06	4.65	300
∞	3.39	8.08	4.66	300

Table 2. Structural bedrock models representative of the path from the epicenters to the city of Rome (Q_α=2.2 Q_β). For the computations with source 3, located in the Alban Hills, the mechanical parameters of the first layer are given in parenthesis.

FIGURE CAPTIONS

Figure 1. Epicenter locations of the events used for the different numerical simulations. The source positions are (1) the epicenter of the January 13, 1915 Fucino earthquake, (2) the Carseolani Mountains, and (3) the Alban Hills.

Figure 2. Lithology and thickness of alluvial sediments in Rome (Ventriglia, 1971; Funiciello et al., 1987; Feroci et al., 1990). The dashed lines indicate the positions of the cross sections, for which numerical modelling is performed.

Figure 3. Two-dimensional models corresponding to the dashed lines shown in Figure 2. Only the part near to the surface is shown, where the 2D model deviates from the horizontally-layered structural models shown in Table 2. The general micro-zonation is explained in the text.

Figure 4. Ratios of the peak ground acceleration, PGA(2D)/PGA(bedrock), and of the Arias Intensity, W(2D)/W(bedrock), obtained for the numerical simulation of the Fucino earthquake (event 1 in Figure 1). They are compared with the damage distribution caused by the January 13, 1915 Fucino earthquake (Fäh et al., 1993). The general micro-zonation is explained in the text.

Figure 5. Maximum and average relative spectral accelerations for the zones defined in Figures 3 and 4, for zero damping and 5% damping.

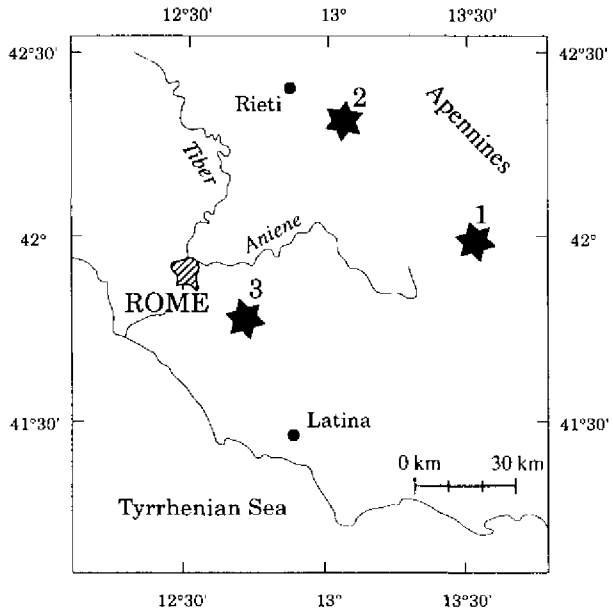
12°30'
13°
13°30'
42°30'
42°
41°30'
Rieti
2
Apennines
Tiber
Aniene
1
ROME
3
Latina
0 km
30 km
Tyrrhenian Sea

Fig.1

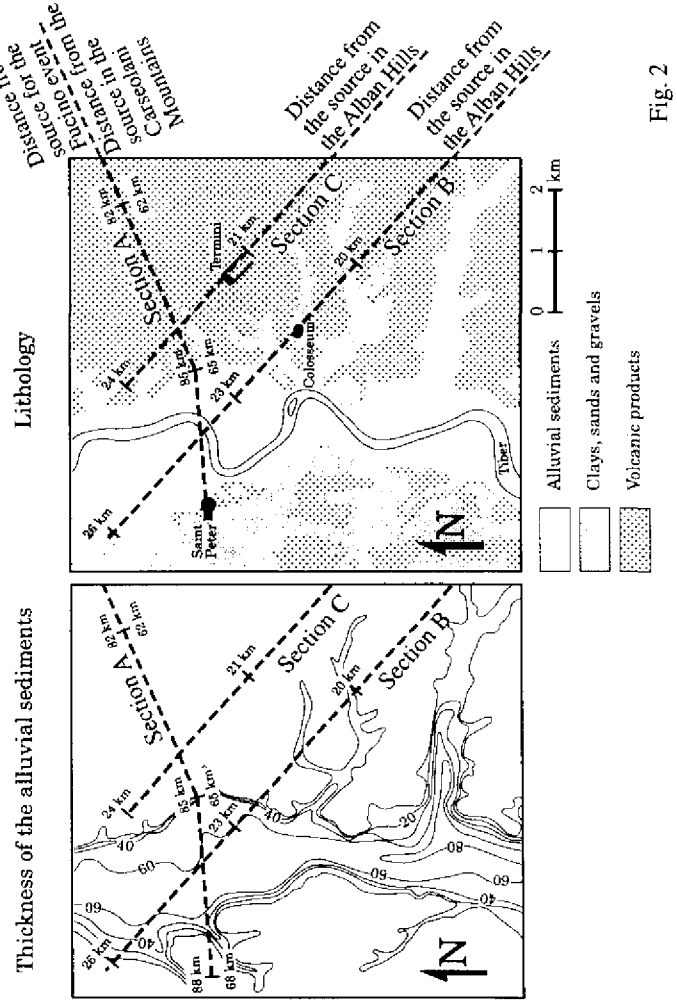
Distance from the source for the Fucino event
Distance from the source in Carseolum Mountains
Distance from the source in the Alban Hills
Distance from the source in the Alban Hills
Lithology
Section A
Section C
Section B
Terminio
Colosseum
Saint Peter
Tiber
N
0
1
2
km
Alluvial sediments
Clays, sands and gravels
Volcanic products
Thickness of the alluvial sediments
Section A
Section C
Section B
N

Fig. 2

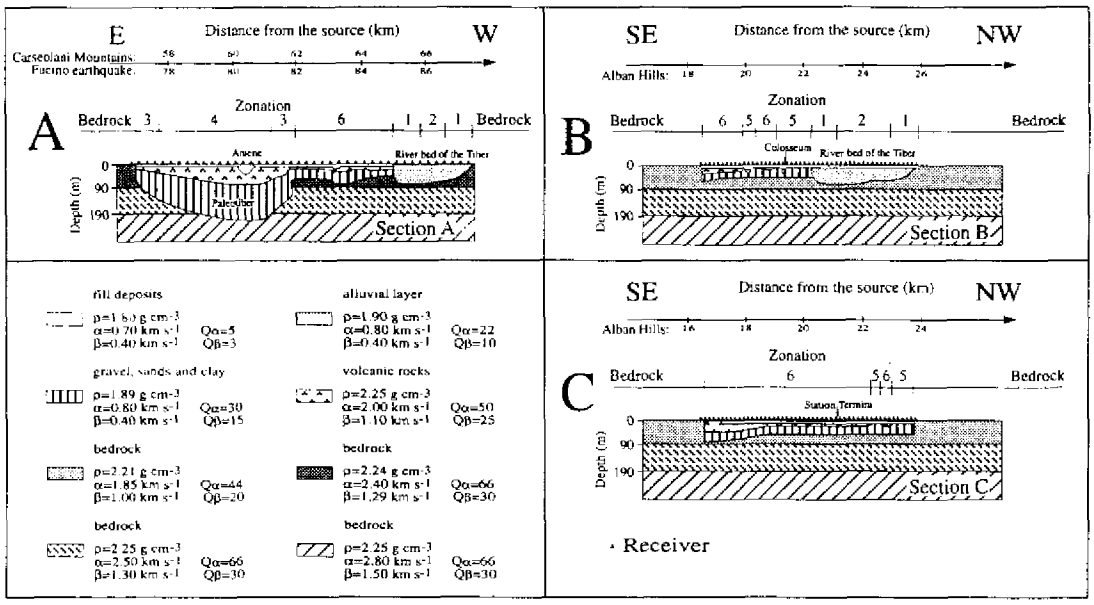
E
Distance from the source (km)
W
Carseolani Mountains
Fucino earthquake
Zonation
A
Bedrock 3 4 3 6 1 2 1 Bedrock
Arsene
River bed of the Tiber
Paleovalley
Depth (m)
Section A
SE
Distance from the source (km)
NW
Alban Hills
Zonation
B
Bedrock 6 5 6 5 1 2 1 Bedrock
Colosseum
River bed of the Tiber
Section B
fill deposits
alluvial layer
gravel, sands and clay
volcanic rocks
bedrock
bedrock
bedrock
bedrock
SE
Distance from the source (km)
NW
Alban Hills
Zonation
C
Bedrock 6 5 6 5 Bedrock
Station Termini
Section C
Receiver

Fig. 3

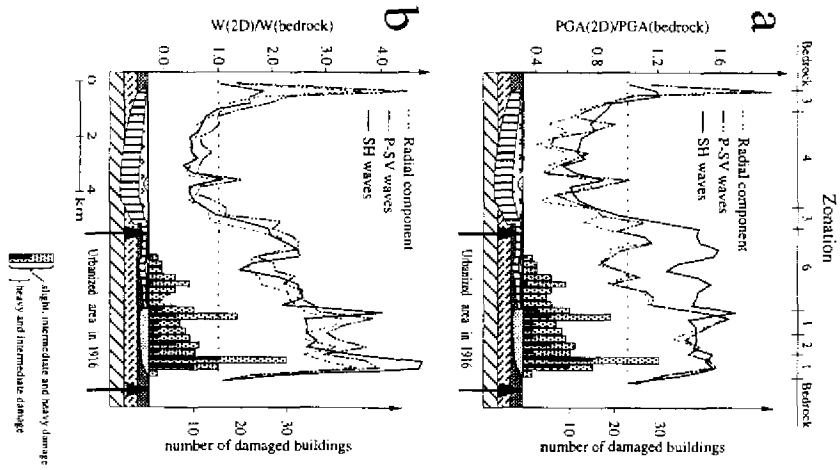
b
W(2D)/W(bedrock)
Radial component
P-SV waves
SH waves
km
Urbanized area in 1916
slight, intermediate and heavy damage
heavy and intermediate damage
number of damaged buildings
a
PGA(2D)/PGA(bedrock)
Radial component
P-SV waves
SH waves
Urbanized area in 1916
number of damaged buildings
Zonation
Bedrock

Fig. 4

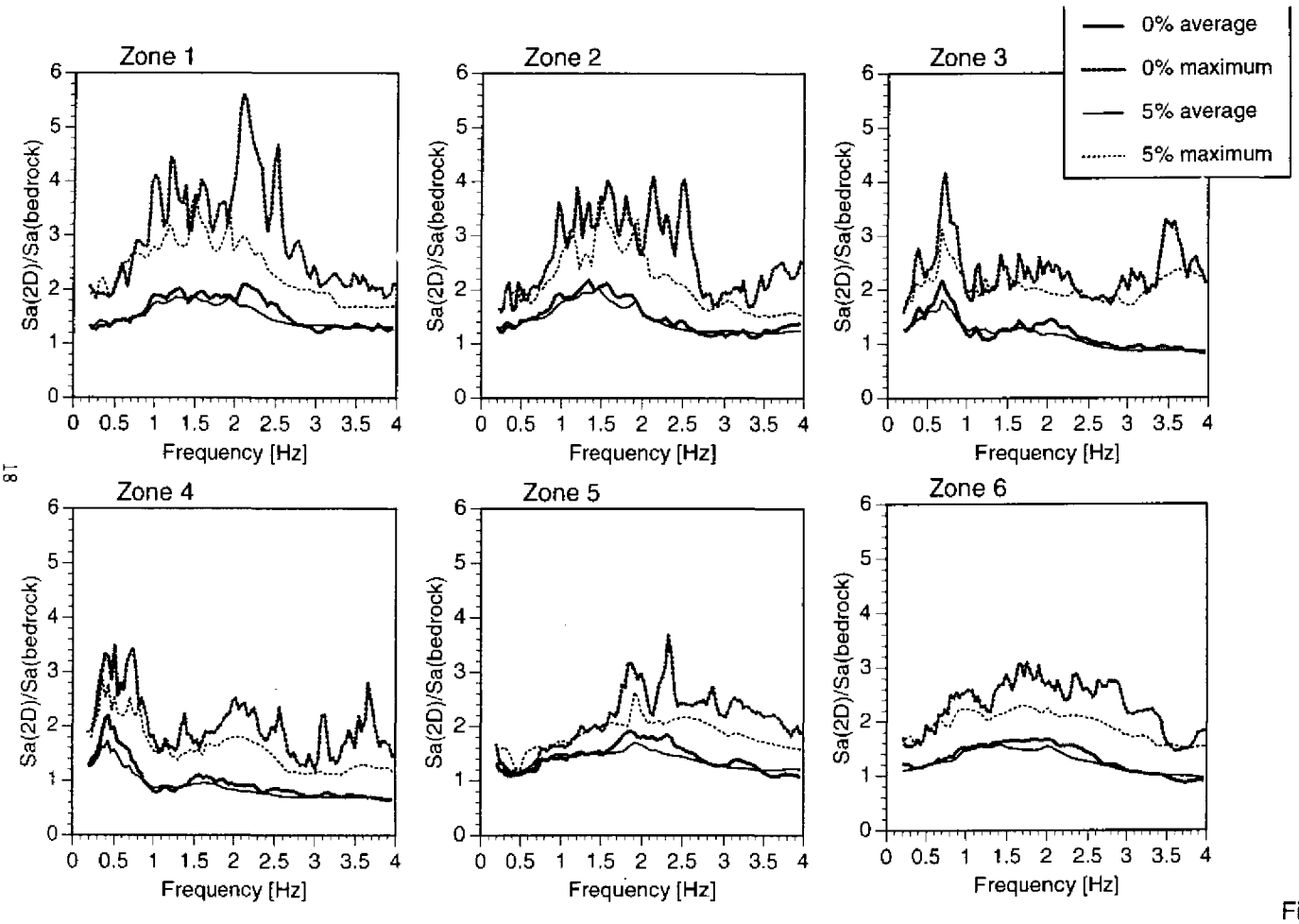
Zone 1
Zone 2
Zone 3
Zone 4
Zone 5
Zone 6
0% average
0% maximum
5% average
5% maximum
Sa(2D)/Sa(bedrock)
Frequency [Hz]
0
1
2
3
4
5
6
0.5
1.5
2.5
3.5

Fig.5